Korean J. Chem. Eng., 36(6), 929-941 (2019)
DOI: 10.1007/s11814-019-0266-2

pISSN: 0256-1115
eISSN: 1975-7220

Optimization and experimental investigation in bottom inlet cyclone separator for performance analysis

Seenivasan Venkatesh*,†, Murukesan Sakthivel, Muthukumar Avinasilingam***, Subramanian Gopalsamy****, Eswaran Arulkumar*****, and Hari Prasanth Devarajan******

*Mechanical Engineering, Sri Eshwar College of Engineering, India
**Mechanical Engineering, Anna University Regional Campus, Coimbatore, India
***R&D Department, Rane TRW, Chennai, India
****R&D Department, Quest Global, Bangaluru, India
*****R&D Department, Focus-R, Chennai, India
******Programming Division, Infosys, Bangaluru, India
(*Received 6 October 2018 • accepted 8 April 2019*)

Abstract−The chemical engineering industries are utilizing the bottom inlet cyclone separator with venturi for separating the particles from an air/gas medium. For improving the performance of this equipment, important geometrical features such as venturi inlet width, total height of the cyclone and body height of the cyclone are considered for optimization. Central composite design was used in response surface methodology (RSM) to fit the regression equation. This regression equation was evaluated by analysis of variance (ANOVA). Then, this polynomial equation was optimized by particle swarm optimization (PSO) for minimizing the cut-off diameter. These optimized results were compared with genetic algorithm (GA) results. Based on this optimized result, an experimental setup was created for validation purpose. The experimental results were compared with GA and PSO results. A good agreement was obtained between these results. The magnesium particles were utilized for predicting the cut-off diameter of the new design. The Stokes number of this new design was less when compared with the mathematical model. The new design gives better performance when compared with the mathematical model. The numerical simulation was executed for predicting the particle collection efficiency, cut-off diameter and flow pattern inside the cyclone. The results were compared with the mathematical model and venturi inlet tangential entry cyclone.

Keywords: Mathematical Model, Cut-off Diameter, Response Surface Methodology, Particle Swarm Optimization, Genetic Algorithm, CFD

INTRODUCTION

Cyclone separators are broadly utilized for the separation of particles from gas or fluid medium, as well as in industrial processes such as chemical engineering, aerosol sampling, pharmaceuticals, foundry processing and mineral processing industries, because of geometrical simplicity and flexibility [1]. Usually, cyclone separators are classified according to inlet arrangement such as tangential inlet, helical inlet, involute inlet, axial inlet and bottom inlet. In the bottom inlet, the particle enters into the cyclone through a tangential inlet structure located at the body's bottom (just over the conical section) and departs through a tangential outlet at the top of the cyclone's body [2]. Many researchers utilized different approaches to improve the separation efficiency of tangential inlet and axial flow cyclone separators. Ray et al. [3] adopted a post cyclone above the vortex finder region for capturing the particles' escape through the outlet port. Liu et al. [4] examined the separation effects of the cyclone separator based on the unusual provision of the particles at the inlet. Bernardo et al. [5] investigated the effect of inlet section angles on collection efficiency. Moreover, that research confirms that the collection efficiency of the cyclone was increased by angular inlet section.

Chuah et al. [6] studied the effect of different cone dimensions on the collection efficiency of small aero cyclones. Diao et al. [7] investigated the axisymmetric square cyclone separator by computational fluid dynamics approach, and results have been compared with single and double inlet cyclone separator. Kim and Lee [8] experimentally considered the effect of vortex finder dimension on cyclone separator. In addition, that research concludes that decreasing the vortex finder diameter increases the collection efficiency. Qian et al. [9] adopted a prolonged vertical tube at the bottom of a cyclone separator that increases the separation efficiency of this equipment. Jiao et al. [10] implemented a rotational classifier in the vortex finder region to enhance the collection efficiency. Park et al. [11] proposed the optimum sizing and features of the cyclone separator for separating the solid CO_2 from gaseous COF_2. Elsayed and Lacor [12] examined the effect of dust outlet geometry on performance and flow pattern in a cyclone separator. Avci and Karagoz [13] investigated the effects of flow and geometrical parameters on the performance of the cyclone. Martignoni et al.

†To whom correspondence should be addressed.
E-mail: venkatesme2014@gmail.com

[14] examined the effect of symmetrical inlet and a volute scroll outlet section in an experimental cyclone.

To enhance the cyclone performance, several researchers go behind various scientific approaches such as optimization techniques and design of experiment techniques. Zhao and Su [15] utilized artificial neural networks and dynamically optimized search technique for modeling the pressure drop coefficient. Elsayed and Lacor [16] used response surface methodology and downhill simplex method to minimize the pressure drop and increase the collection efficiency of a cyclone separator. Safikhani et al. [17] used group method of data handling neural networks and multi-objective genetic algorithm to reduce the pressure drop and increase the performance. Pishbin and Moghiman [18] optimized the seven geometrical parameters of the cyclone separator by using genetic algorithm to increase the efficiency. To predict the nonlinear relationship between the pressure drop, cut-off diameter and geometrical parameters, the artificial neural network was used. Also, to minimize the pressure drop and minimize the cut-off diameter, genetic algorithm was used [19]. Recently, Kumar and Jha [20] utilized multi-objective optimization for improving the performance of the cyclone separator by altering the geometric parameters of the vortex finder. Luciano et al. [21] examined the series based arrangement of cyclone separators by COBYLO optimization method for enhancing the collection efficiency. Brar and Elsayed [22] analyzed the performance of cyclone separator with eccentric vortex finder by genetic algorithm and artificial neural network approach. For improving the performance of cyclone separator, the geometric parameters of the cyclone separator have been optimized by surrogate model optimization approach [23].

The literature survey concludes that most of the researchers considered only tangential inlet (inlet at the top of the cyclone body) and axial inlet cyclone separators for performance analysis. Optimization techniques such as genetic algorithm and Nelder mead optimization have been used to increase the performance of cyclones. Artificial neural networks and response surface methodology have been used for fitting the objective functions and nonlinear relationship in past decades. In this research, a venturi type inlet was adopted with bottom inlet cyclone separator. Also, response surface methodology and particle swarm optimization techniques have been used to minimize the cut-off diameter of the particle. Then, this optimized result is compared with the results of genetic algorithm. Also, an experimental setup was created based on that optimized parameters for validation purpose. Moreover, these results were compared with the venturi inlet tangential entry cyclone separator.

MATHEMATICAL MODEL

Initially, a mathematical model was created for predicting the cut-off diameter of the particles in bottom inlet cyclone separator. In this model, a venturi inlet is attached to the bottom inlet of the cyclone separator to increase the particle loading capacity. In this mathematical model, the dimensions of the venturi are based on Viswanathan's [24] model. The dimensions of the cyclone separator were created based on Stairmand [25] model, except total height and body height. These two parameters are initially assumed because the inlet of the cyclone is not normal. Here, the inlet is located just above the cone section. The layout diagram of the mathematical model is shown in Fig. 1. The dimensional parameters of this model are given in Table 1. The particle cut-off diameter of this mathematical model can be estimated by Eq. (1) and Eq. (2). The calculated cut-off diameter (X_{50}) of the particle is 9.129×10^{-6} m at a velocity of 3.3 m/s. Then, cut-off diameter based Stokes number is computed by Eq. (3). The value of Stokes number is 0.01422 at a velocity of 3.3 m/s. For calculating the cut-off diameter and Stokes number of this model, the input parameters such as particle density (ρ_p) is 1,740 kg/m^3, gas density (ρ_g) is 1.225 kg/m^3, viscosity (μ) is 1.78×10^{-5} kg/ms are considered.

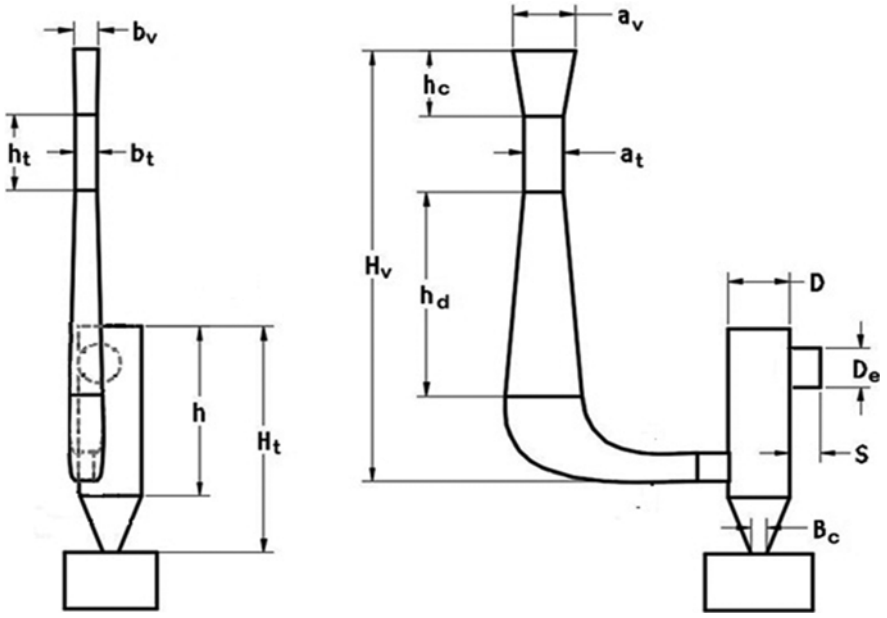

Fig. 1. Layout diagram of bottom inlet cyclone separator.

Table 1. Dimensions of the bottom inlet cyclone separator

S. No.	Parameters	Dimension (m)
1	Cyclone diameter (D)	0.105
2	Outlet diameter (D_e)	0.0525
3	Total height (H_t)	0.6
4	Body height (h)	0.4
5	Cone tip diameter (B_c)	0.0394
6	Inlet length of venturi (a_v)	0.125
7	Inlet width of venturi (b_v)	0.075
8	Convergent section height (h_c)	0.12
9	Divergent section height (h_d)	0.37
10	Throat section height (h_t)	0.125
11	Throat length (a_t)	0.07
12	Throat width (b_t)	0.03
13	Total height of the venturi (H_v)	0.74

$$\text{Cut-off diameter } (X_{50}) = \left[\frac{9\mu b_v}{2\pi N_e V_i(\rho_p - \rho_g)}\right]^{0.5} \quad (1)$$

$$\text{Number of turns } N_e = \frac{1}{a_v}\left[h + \frac{H_t - h}{2}\right] \quad (2)$$

$$\text{Stokes numbe } (Stk_{50}) = \frac{\rho_p X_{50}^2 V_i}{18\mu D} \quad (3)$$

RESPONSE SURFACE METHODOLOGY

RSM, which is a compilation of statistical and mathematical techniques, is helpful for modeling and analysis of complex problems containing several variables [26]. It is also used to solve multivariate problems. Recently, this technique was adopted in the field of manufacturing and engineering design. In this research, the Minitab 16 statistical software was used to perform the RSM analysis. Based on the literature survey report, three parameters are mostly associated with cut-off diameter and performance of the cyclone. The parameters are total height (H_t) of the cyclone, cylindrical body height (h) of the cyclone and inlet width of the venturi (b_v), which is attached with the inlet of cyclone separator. Based on these three parameters, the experimental run was planned. RSM has two types of design: Central composite design (CCD) and Box-Behnken design. We used CCD method to plan the design matrix. After creating this design matrix, the response parameter such as particle cut-off diameter was predicted for each combination of parameters. After that, the full quadratic equation was created by regression analysis to fit the objective function. The universal quadratic equation utilized in the RSM is as follows:

Table 2. Levels of the variables

Variables	Low (m)	High (m)
Total height of the cyclone (H_t)	0.5	0.6
Body height of the cyclone (h)	0.35	0.4
Venturi inlet width (b_v)	0.04	0.075

$$Y = \beta_0 + \Sigma_{i=j}^{7}\beta_i X_i + \Sigma_{i=j}^{7}\beta_{ii} X_i^2 + \Sigma\Sigma_{i<j}\beta_{ij} X_i X_j \quad (4)$$

1. Central Composite Method

In this work, the full factorial central composite design (CCD) method was used to create the design matrix. Moreover, CCD type of design was selected to run the design matrix from the design

Table 3. CCD matrix with actual variables and cut-off diameter

S. No.	Total height of the cyclone (H_t) (m)	Body height of the cyclone (h) (m)	Venturi inlet width (b_v) (m)	Cut-off diameter (μm)
1	0.55	0.35	0.0575	8.425944
2	0.5	0.4	0.04	7.027723
3	0.5	0.35	0.075	9.902094
4	0.515	0.355	0.045	7.581454
5	0.6	0.4	0.045	7.07151
6	0.5	0.4	0.075	9.623106
7	0.6	0.4	0.075	9.12928
8	0.53	0.36	0.05	7.901252
9	0.545	0.365	0.055	8.195332
10	0.5	0.375	0.0575	8.545467
11	0.5	0.35	0.04	7.231467
12	0.56	0.37	0.06	8.467204
13	0.55	0.375	0.04	6.932103
14	0.6	0.35	0.075	9.366443
15	0.575	0.38	0.065	8.696828
16	0.6	0.35	0.04	6.840283
17	0.59	0.385	0.07	8.93208
18	0.55	0.4	0.0575	8.201211
19	0.6	0.375	0.0575	8.095385
20	0.55	0.375	0.075	9.492173

menu bar in Minitab software. There are three parameters considered, which are associated with particle cut-off diameter such as the total height (H_t) of the cyclone, cylindrical body height (h) of the cyclone and inlet width of the venturi (b_v). Therefore, three factors option was selected from the number of factors menu bar. The maximum available response surface design was 20 runs for three factors in the CCD method. Therefore, the maximum number of runs was selected as 20 for getting the most accurate result.

The number of replicates and alpha values are given as 1 and 1.682, respectively, in the design menu. For creating the design matrix, the factor levels, such as low and high values, are given for the above-said three parameters in the factor input menu bar. The factor levels are shown in Table 2. Subsequently, the CCD matrix was generated for those two levels and three parameters. It has 20 combinations. The response parameter such as particle cut-off diameter can be calculated for that 20 runs by Eq. (1) and Eq. (2). The CCD matrix with cut-off diameters is shown in Table 3. This response surface design was analyzed by creating the regression coefficient. Here, the confidence level was set at 95% ($P<0.05$) for all tests. The predicted R^2 value was 99.95% or 0.9995. It indicates that the created mathematical model is very efficient. The regression equation was generated based on the regression coefficient value, which is given in Eq. (5). In this equation, X(1), X(2) and X(3) are corresponding to total height of the cyclone (H_t), cyclone

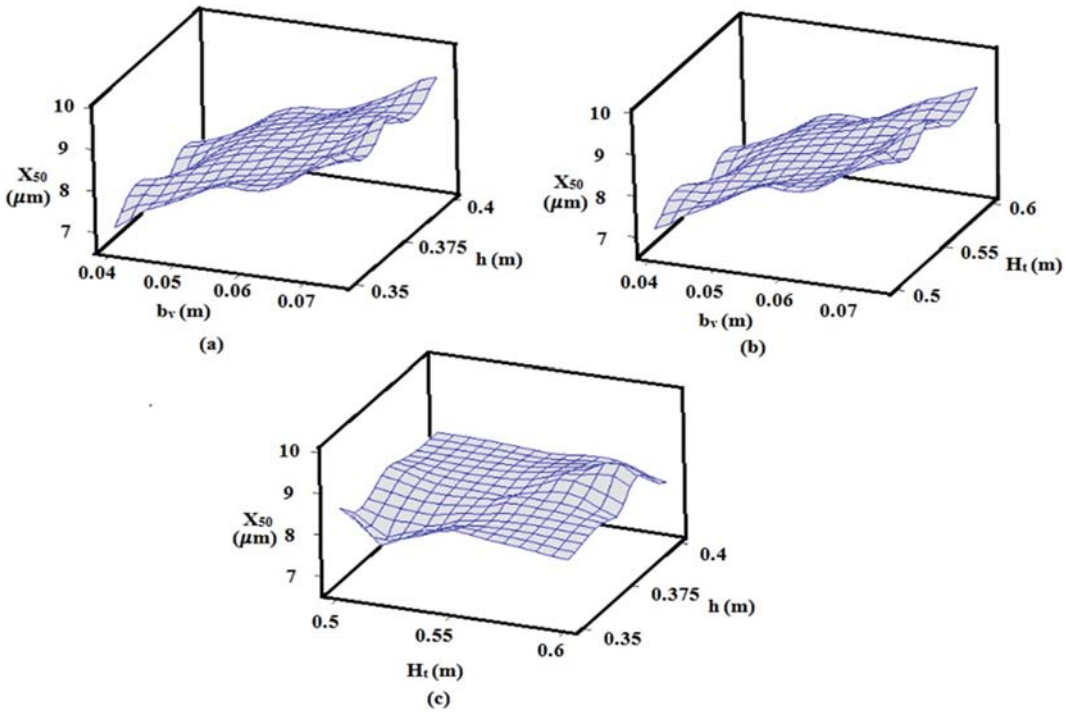

Fig. 2. Surface plots (a) cut-off diameter vs venturi-inlet width and body height (b) cut-off diameter vs venturi-inlet width and total height (c) cut-off diameter vs Total height and body height.

Table 4. ANOVA table for cut-off diameter

Source term	Degrees of freedom	Sequential sum of squares	Adjusted sum of squares	Adjusted mean squares	F-ratio	P-value
Regression model	9	18.3634	18.3634	2.04037	138642.19	0.000
Total height (H_t)	1	0.0566	0.0009	0.00091	61.77	0.000
Body height (h)	1	0.0005	0.0002	0.00021	14.28	0.004
Venturi inlet width (b_v)	1	18.2588	0.1173	0.11732	7971.88	0.000
H_t*H_t	1	0.0058	0.0002	0.00019	12.74	0.005
h*h	1	0.0020	0.0000	0.00004	2.45	0.149
b_v*b_v	1	0.0263	0.0268	0.02675	1817.74	0.000
H_t*h	1	0.0004	0.0007	0.00073	49.45	0.000
H_t*b_v	1	0.0107	0.0102	0.01018	691.50	0.000
h*b_v	1	0.0024	0.0024	0.00243	165.14	0.000
Residual error	10	0.0001	0.0001	0.00001		
Total	19	18.3635				

body height (h) and venturi inlet width (b_v).

$$Z=8.44022-0.00865*X(1)-0.01067*X(2)+0.14697*X(3)+0.00001*X(2)*X(2)-0.00032*X(3)*X(3)+0.00001*X(1)*X(2)-0.00004*X(1)*X(3)-0.00004*X(2)*X(3); \quad (5)$$

2. Analysis of Variance (ANOVA)

The competence of the developed mathematical quadratic model was checked by analysis of variance (ANOVA). The F-Test was conducted by this analysis for individual variables and interactions. The developed ANOVA results are shown in Table 4. This result indicates that the F-test values for linear, square and interaction variables are greater than P value. Moreover, the P-values for each linear, square and interactions are less than 0.05 ($P<0.05$) except the square term of body height. It means the confidence level of the developed model is 95% and indicates that developed model is within the confidence limit. In addition, it shows that all the individual variables, interaction variables and square variables have produced a significant effect. But the square term of body height produced an insignificant effect ($P>0.05$). All other parameters (except the square term of body height) produced a significant effect on the cut-off diameter of the particles. These results are clearly indicating that the developed quadratic polynomial model has excellent fitness on particle cut-off diameter.

PARTICLE SWARM OPTIMIZATION

Particle swarm optimization (PSO), developed by Eberhart and Kennedy in 1995, is a population based optimization technique. This optimization starts with a population of arbitrary solution. Then it searches the optimum solution by updating the generations. This optimization is working based on a group of birds searching food randomly in a place. Here every bird is considered as a particle and food is considered as an optimum problem solution within a searching space [27]. Every variable is considered as a particle, and the response parameter is considered as an optimum problem solution. In this work, the variables such as venturi inlet width, total height of the cyclone and body height of the cyclone are considered as a particle and cut-off diameter is considered as problem solution. In this optimization, the particles or variables are following the current optimum particles. For updating the generations, at first the problem starts with a set of arbitrary particles. From these random generations, the optimized one is identified by updating the current generations. Moreover, each particle is updated by two best values such as 'pbest' value and 'gbest' value. The 'pbest' value is obtained from particles. The 'gbest' value is obtained from the population. After finding these two values, the position and velocity of the particle in current generations are updated by the following formulas [27].

$$y_{ij}^{n}=y_{ij}^{n}+v_{ij}^{n+1} \quad (6)$$

$$v_{ij}^{n+1}=wv_{ij}^{n}+c_1R_1(P_{ij}^{n}-y_{ij}^{n})+c_2R_2(g_{ij}^{n}-y_{ij}^{n}) \quad (7)$$

$$w(n)=w_L+\frac{w_U-w_L}{I_U}x(I_U-n) \quad (8)$$

where c_1 and c_2 are the learning factors, R_1 and R_2 are the random numbers, y_i^n is the position vector, v_i^n is the velocity vector, w is the inertia weight, P_{ij}^n and g_{ij}^n are pbest and gbest values, w_U and w_L are the upper and lower limits of inertia weight, I_U is the maximum number of iterations and n is the current number of iterations.

1. PSO Calculation Procedure

Step 1: Initialize the position and velocity of the 'n' number of particles within a population randomly. Then search the 'gbest' value among this initial 'pbest' value of all particles.

Step 2: Estimate the fitness function value for each particle. If fitness value is better than 'pbest' value then set this fitness value as a current 'pbest' value.

Step 3: Again search the 'gbest' value among this current 'pbest' value. Then compare this new 'gbest' value with the previous one. If the current iteration is better than the previous value, then set this value as a new one. If not, previous

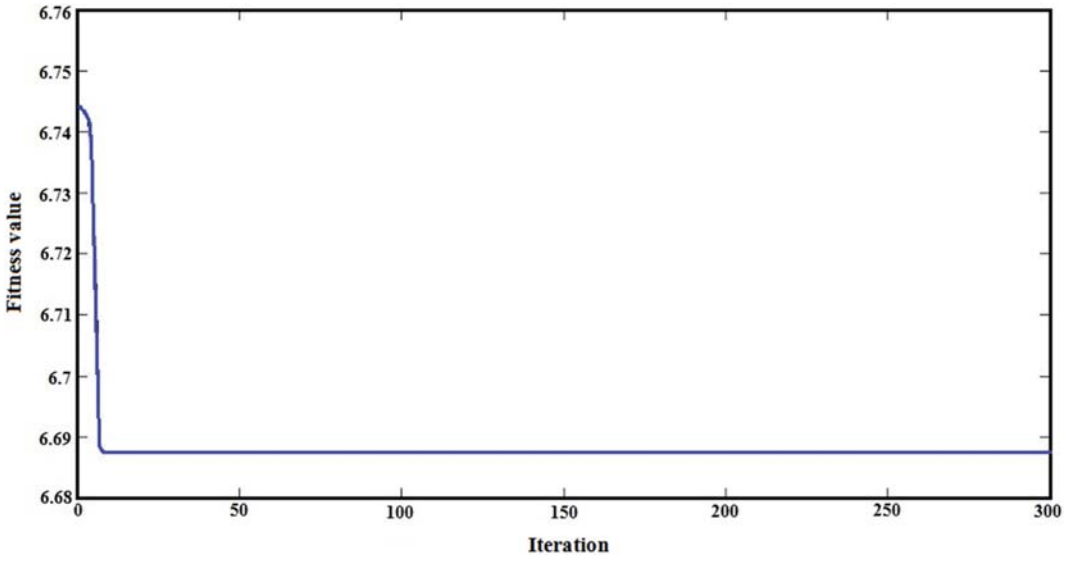

Fig. 3. Fitness value vs iteration.

'gbest' value remains unchanged.

Step 4: The position and velocity vectors of the particle are estimated by Eq. (6) and Eq. (7).

Step 5: Stop the calculation if the iteration reaches its maximum value. If not, then continue until it reaches a maximum value (go to step 2).

Step 6: End.

2. PSO Parameters Settings and Results

We used MATLAB 7.10.0 (R2010a) for optimization. Initially, the objective function was created based on the regression equation which is given in Eq. (5). This objective function was written in m-file of the MATLAB software. After creating this m-file in MATLAB, the PSO parameters were given to optimization. The number of variables was given as 3. Number of population was set at 100. Total number of iterations was given as 300. Learning factors such as c_1 and c_2 were set as 2. The range of the random number was given as 0 to 1. The upper and lower limits of the inertia weight were 0.9 and 0.4, respectively. The upper limits of the variables were 600, 400, and 75, respectively. The lower limits of the variables were 500, 350 and 40, respectively. After setting these parameters, the optimization was run. The solution converged in 300 iterations. The updated pbest and gbest value was 6.6875. The number of iterations versus fitness function plot is shown in Fig. 3. This plot confirms that the fitness value terminated in 6.6875. The updated pbest and gbest variables are 600, 350 and 40. From this optimized variable, the cut-off diameter and Stokes number can be calculated by Eq. (1), Eq. (2) and Eq. (3). The optimized cut-off diameter and Stokes number is 6.84×10^{-6} m and 0.007986, respectively.

GENETIC ALGORITHM

Genetic algorithm (GA) is a nontraditional random search algorithm developed by Holland in 1960. It has been used in many industries and engineering fields to solve complex problems. It is also used in engineering design, parameter optimization in machining, reducing the time, energy and manufacturing processes in various industrial processes [28]. In this work, GA was utilized to optimize the three important geometric features of cyclone separator. The main objective of this optimization is reducing the particle cut-off diameter by modifying those three variables, which is clearly mentioned in the previous section. Moreover, GA results were compared with the PSO results to check the accuracy of this optimization process. MATLAB 7.10.0 (R2010a) was used for GA optimization.

1. GA Settings in MATLAB

We developed the polynomial quadratic equation by response surface methodology. The significance of this mathematical equation was validated by ANOVA technique. For GA optimization, an objective function was written in m-file based on that quadratic equation, which is given in Eq. (9). The created m-file fitness function is as follows:

```
1. Function Z=f (X);
2. Z=8.44022−0.00865* X(1)−0.01067* X(2)+0.14697* X(3)
     +0.00001* X(2) * X(2)−0.00032* X(3) * X(3)
     +0.00001* X(1) * X(2)−0.00004* X(1) * X(3)
     −0.00004* X(2) * X(3);
```

(9)

After creating the objective function in m-file, the fitness function and number of variables are given in the problem menu bar. The type of the population is selected as double vector type and the size of the population is specified as 30. The uniform creation function is selected in population. Then, initial and final range of the parameters such as total height of the cyclone (H_t), cyclone body height (h) and venturi inlet width (b_v) is given as [500,350,40;600,400,75],

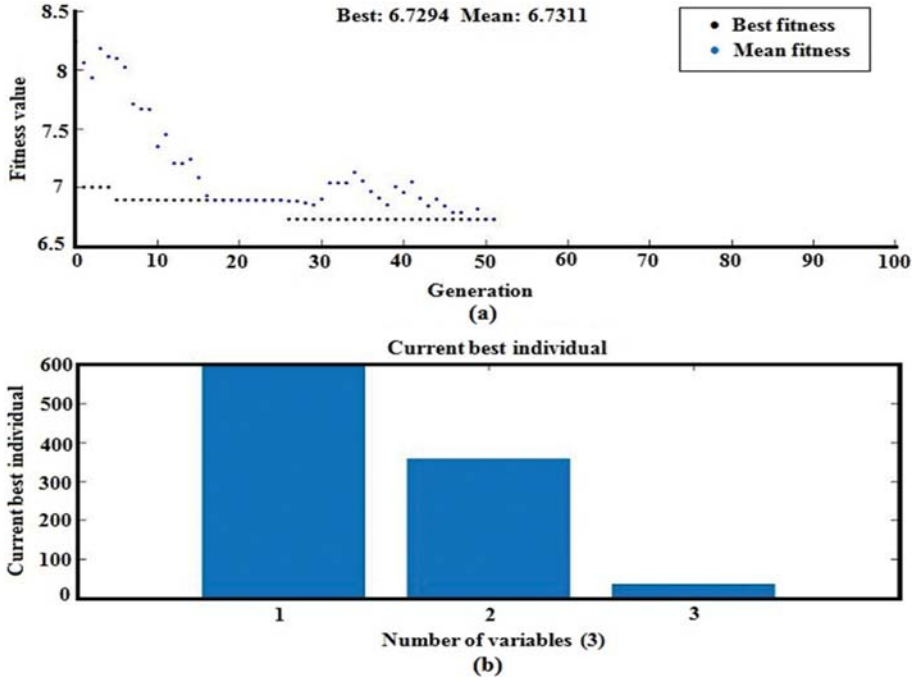

Fig. 4. (a) Generation vs fitness value, (b) number of variables vs current best individual.

respectively. The rank type scaling function was set in a fitness scaling menu bar. The uniform selection function was set in the selection criteria. In the reproductive function, the elite count value and the crossover fraction value were set at 2 and 0.8, respectively. Also, the mutation rate was set as user default value, which is a 0.01 and mutation function is uniform. The single point type was preferred from crossover function. In addition, the migration direction was given as forward and its fractional value was 0.2 and its interval was 20. The initial penalty and penalty factor were set as user default. The generation value was set as 100 and stall generation value was set as 50. The function and nonlinear constrained tolerance was given as $1e^{-6}$. The best fitness and best individual function was elected from plotting function. The GA optimization was initiated after setting these parameters. The solver terminates the iteration after reaching the objective function value. The plots such as generation versus a fitness value and number of variables versus current best individuals were plotted as shown in Fig. 4. From these plots, the best fitness value is identified as 6.7294, and the mean fitness value is 6.7311. The optimized three geometric parameters are 596.19, 359.19 and 40.108, respectively, which are identified from current best individuals. Based on these three optimized parameters, the cut-off diameter of the particle was estimated which is 6.83×10^{-6} m. The estimated Stokes number was 0.007962.

EXPERIMENTAL VALIDATION

The experimental setup was created based on the optimized results, which is shown in Fig. 5. In addition, the magnesium particle was used to predict the cut-off diameter in this research. In this setup, a vibratory type particle feeder was used to feed the magnesium particles through the inlet of the venturi. This vibratory feeder delivers the particles in the range of 800 g/min. The density of the magnesium particle was 1,740 kg/m^3. The average mean particle size range utilized in this research was 7 μm. The size of the particle is measured by the particle sizer for verification purpose. The centrifugal suction blower was used to draw the magnesium particles from the inlet of the venturi. This blower is attached at the tangential outlet of the cyclone separator. It has a suction inlet port at the center axis and its outlet is tangential to the impeller. It receives suction air through the center axis of the impeller, and it delivers to the tangential outlet. This blower has 0.046 m^3/s suction capacity. The inlet velocity was measured by anemometer at the inlet of the venturi. The measured inlet velocity was 3.9 m/s.

Fig. 5. Experimental setup.

In addition, for measuring the pressure drop between the inlet of the venturi and the outlet of the cyclone separator, two vacuum gauges were used. The unit of the gauges is in water columns. The measured pressure drop value was 32 mm of water columns or 313.8 N/m^2. The bottom inlet cyclone with venturi was fabricated by the galvanized cast iron, sheet metal with the thickness of 2 mm. The size of the particle collection box was 200×150×150 mm, which is attached at the bottom of the cyclone separator to collect the magnesium particles. For predicting the cut-off diameter or 50% of the collection efficiency, 1 kg of magnesium particles was injected by the particle vibratory feeder. The size dependent efficiency or particle cut-off diameter was predicted with the help of particle counter instruments. Based on the particle counter results, 49.6% of the particles were collected in the collection box, and remaining particles escaped to the atmosphere thorough the outlet of the blower. This result confirms that the cut-off diameter of the particle was 7 μm and its Stokes number was 0.008363. The cut-off diameter of the mathematical model was 9.129 μm. It shows that the cut-off diameter of the optimized model is less when compared with the mathematical model.

NUMERICAL SIMULATION

1. Grid Generation

We used SolidWorks software for creating a solid model for the mathematical model and optimized new design. These solid models convert to IGS file formats for the numerical simulation. Afterwards, the grid was generated by using the finite volume method. The conditions used to generate the grid are given in Table 5. Based on this condition a fine mesh was generated, which is shown in Fig. 6. The created nodes and elements of the mathematical model are 738732 and 665243, respectively. The created nodes and elements of the new model are 726242 and 647235.

2. Mesh Quality Inspection by Mesh Metrics

Generally, in Ansys Fluent the quality of the mesh is validated by three methods: mesh metric evaluation, grid independence study and grid convergence index. The first method is directly available in Ansys Fluent mesh module. By this method the mesh quality is validated easily and fast. But other methods are needed in some

Table 5. Conditions for mesh generation

Parameters	Mathematical model	New design
	Choice/Values	Choice/Values
Meshing method	Cut-cell	Cut-cell
Relevance center	Fine	Fine
Curvature normal angle	18°	18°
Minimum size	0.000021 m	0.000025 m
Maximum size	0.0024 m	0.0018 m
Growth rate	1	1
Transition ratio	0.272	0.272

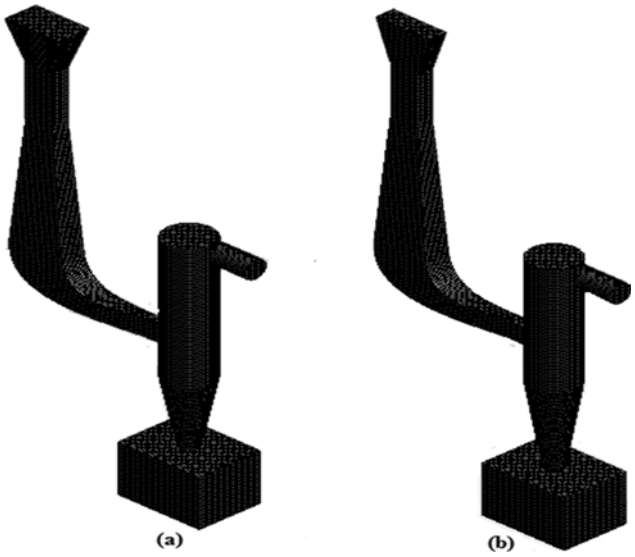

Fig. 6. (a) Mesh for mathematical model (b) mesh for optimized model.

mathematical calculation and simulation in each step, so it takes more time for validating the mesh. For this reason, in this work, the mesh metric method was used. The following results were obtained from this test. The element quality results show that the average elements metrics value for the mathematical model and the new model is 0.976 and 0.977, respectively, at the highest number of elements. The aspect ratio results give the average metric values for both models as 1.18 and 1.172 at the highest number of elements. The Jacobian ratio values for the both models are 1.043 and 1.039. These results indicate that the produced mesh quality is excellent.

3. Boundary Conditions

The velocity inlet boundary condition is given at the inlet of the attached venturi in the bottom inlet cyclone. The velocity magnitude is given as 3.3 m/s for mathematical model and 3.9 m/s for the optimized model. The pressure outlet boundary condition is set in the outlet of the cyclone separator. The turbulent intensity and turbulent viscosity ratio are 5% and 10, respectively, for both models. Further, no slip wall boundary condition is given for the remaining walls of the bottom inlet cyclone separator. The wall roughness constants were set at 0.5 for both models. The density of the air was set as 1.225 kg/m^3. The viscosity of the air was set at 1.75×10^{-05} kg/ms.

4. Turbulence Model and Simulation Schemes

The numerical simulation was done by the RSTM approach, which is a most promising model for complex flow problems [29]. The simulation starts with unsteady or transient flow. The pressure-based velocity formulation and linear pressure-strain model was selected in RSTM [30,31]. The gravitational acceleration is given in Y direction as 9.81 m/s^2. For producing the accurate results, the following schemes were selected in CFD, which is shown in Table 6. In the turbulent kinetic energy and turbulence dissipation rate the relaxation factor was set at 0.8. In the Reynolds stress and discrete phase sources the relaxation factor was set at 0.5 [32,33]. The solution was initialized by hybrid initialization. The time step size and the number of time steps were specified as 0.001 s and 5, respectively.

Table 6. Numerical schemes for simulation

Spatial discretization	Selected schemes
Pressure velocity coupling	SIMPLEC
Pressure spatial discretization	PRESTO
Momentum discretization	QUICK
Turbulent kinetic energy	Second order upwind
Turbulent dissipation rate	Second order upwind
Reynolds stress	First order upwind

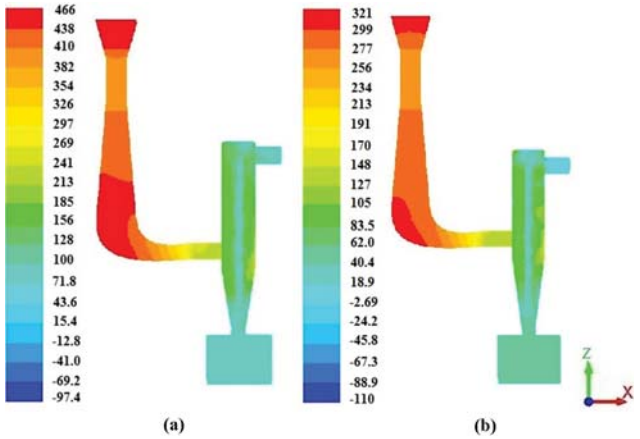

Fig. 7. (a) Pressure contour for mathematical model (b) pressure contour for optimized model (X-Z plane, Sliced at Y=0).

RESULTS AND DISCUSSION

1. Pressure Contours

The static pressure drop contours for bottom inlet cyclone separator with venturi inlet are shown in Fig. 7. The pressure drop reaches the highest value of the venturi region for mathematical and optimized new design cyclones. The minimum pressure drop is in the outlet region of the both models. It is noted that the pressure drop is high on the wall of the venturi and cyclone separator and which gradually decreases towards the central axis of the cyclone. Moreover, the pressure drop between the inlet and outlet of the new design cyclone is less when compared with the mathematical model. It indicates that the particles escaping to the atmosphere are less in a new design cyclone. The pressure drop between the inlet and outlet of the mathematical model was 397.2 N/m^2. The pressure drop between the inlet and outlet of the new design cyclone was 296.8 N/m^2. In addition, the collection box has less pressure drop in a new design cyclone when compared with the mathematical model. Moreover, the pressure drop is less at the top of the cyclone body compared with the conical section of the bottom inlet cyclone. It confirms that the highest number of particles is trapped in the collection box of the new design cyclone compared with the mathematical model.

2. Velocity Contours

Fig. 8 and Fig. 9 show the velocity contours of the mathemati-

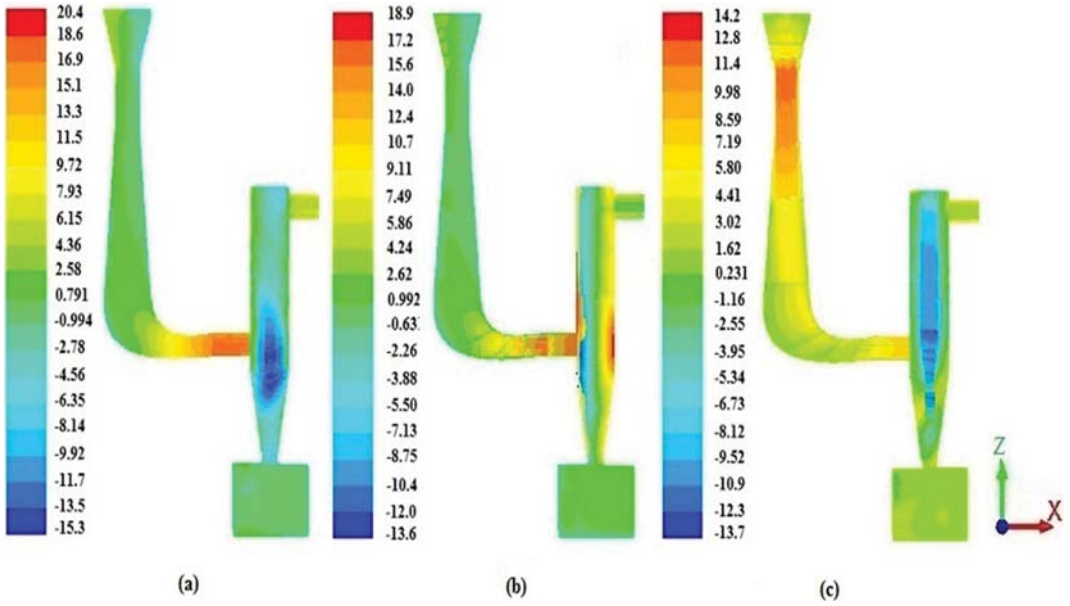

Fig. 8. Velocity contours for mathematical model (a) tangential velocity (b) axial velocity (c) radial velocity (X-Z plane, Sliced at Y=0).

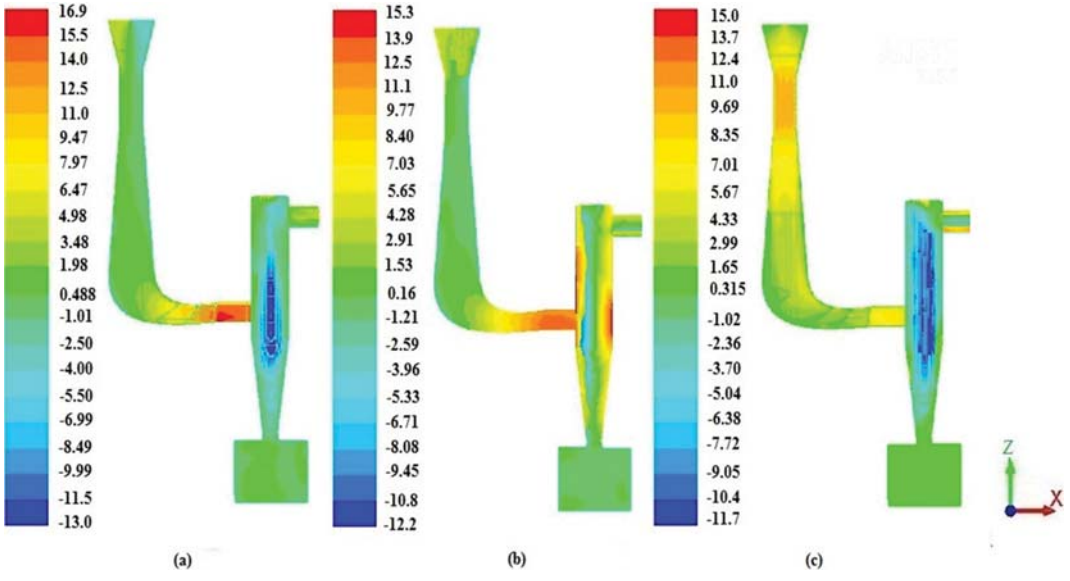

Fig. 9. Velocity contours for new design (a) tangential velocity (b) axial velocity (c) radial velocity (X-Z plane, Sliced at Y=0).

cal model and new design bottom inlet cyclone separator. The tangential velocity is high on the cyclone body outer wall region and it is less at the center axis. The tangential velocity is increased from the center axis to the cyclone cylindrical body section for both models of the cyclone separator. The axial velocity is high in the wall region and is decreasing towards the central axis of the cyclone. In bottom inlet cyclone, the radial velocity is less above the cyclone body wall region. As well, the radial velocity is high in the wall region of the conic section. It proves that the particles are swirling with high velocity in the conical section of the cyclone separator. For to this reason the particles are forced to hit the wall with high centrifugal force. Due to this centrifugal force the particles gradually settle down at the bottom region. Moreover, the tangential, axial and radial velocities of the optimized model is less at the outlet region compared with the mathematical model. It confirms that the particles escaping through the outlet of the cyclone are less in optimized cyclone.

There are two different axial stations considered for creating the x-y plots for tangential, axial and radial velocities. The first section is taken at 125 mm from the top plane of the cyclone separator, and the second section is taken at 200 mm from the top plane of the cyclone separator. The created plots are shown in Fig. 10. These plots are specified that the tangential, axial and radial velocities increased radially from the center axis towards the outer wall region. Moreover, these three velocities are less in the optimum model when compared with the mathematical model. It confirms that the pres-

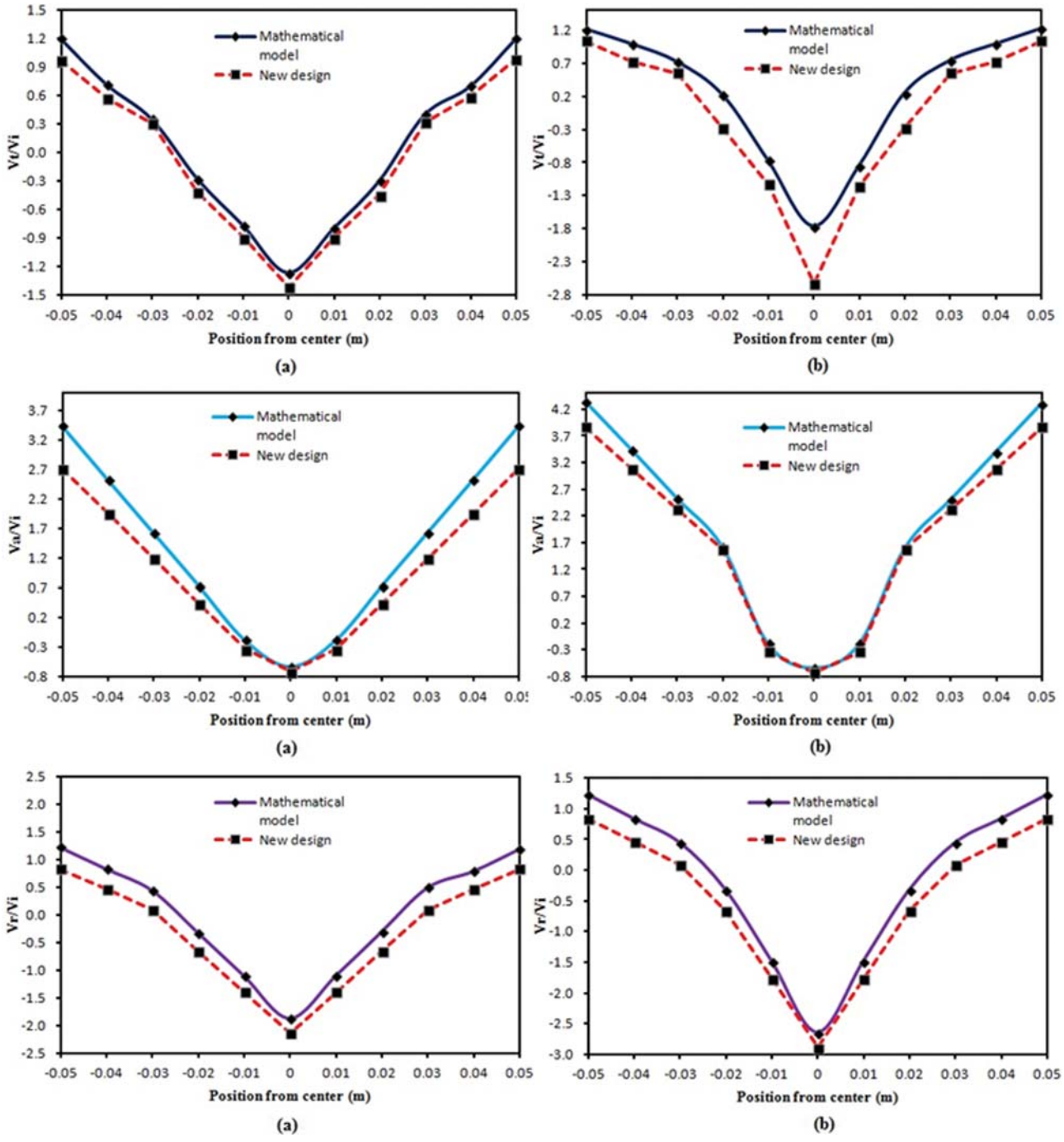

Fig. 10. Radial profiles for Tangential velocity, Axial velocity and Radial velocity from top to bottom. Left to right: (a) Section 1 (b) Section 2.

sure drop in the optimum model is less when compared to the mathematical model. Because, in the cyclone separator, the pressure drop is directly proportional to the velocity. Due to this less pressure drop, more particles easily settle at the bottom of the collection bin in the optimum model compared to the conventional one.

3. Discrete Phase Model Settings

The discrete phase model (DPM) approach was employed in this work for predicting the collection efficiency, cut-off diameter and flow pattern results. The maximum number of steps was set at 500000. The step length factor was set at 5. The particles used in this work are magnesium. The density of the particle was set as 1,740 kg/m^3. The particles were injected from the inlet surface of the venturi; due to this reason the surface injection type was selected from the DPM panel. In addition, for particle injection from inlet surface two options are given: inject using face normal direction and scale flow rate in face area [33]. The mass flow rate was set as for the mathematical model 0.01 kg/s with a velocity of 3.3 m/s. The same mass flow rate was used for the optimized design except inlet velocity. Since, the measured inlet velocity in the inlet of the venturi is 3.9 m/s in the experimental setup. This velocity magni-

tude is given for the new design. The particle diameter distribution was considered as uniform. The particle residence time step was calculated by the following equation:

$$t_{res} = \frac{\text{Effective volume of the cyclone}}{\text{Volume flow rate}} \quad (10)$$

The predicted volume flow rate for the mathematical model and optimized new design at the inlet of the venturi is 0.0327 m^3/s and 0.02028 m^3/s, respectively. The predicted cyclone volumes for the both models are 0.013 m^3 and 0.0125 m^3. The calculated residence time steps for the both models are 0.397 s and 0.616 s, respectively. In CFD, the collection efficiency of the cyclones for a particle diameter was computed by the following equation:

$$\text{Efficiency } \eta(d_p) = \frac{\text{No. of particles trapped}}{\text{No. of particles injected} - \text{No. of particles incomplete}} \quad (11)$$

For predicting the collection efficiency, 3920 particles were injected for the mathematical model at a velocity of 3.3 m/s. For the optimized model, 2100 particles were injected at the velocity of 3.9 m/s. The results are depicted in section 8.5.

4. Flow Pattern Analysis

The flow pattern was developed based on the particle history data obtained from the discrete phase model approach. In this work, the flow pattern was developed based on the particle size of 7 μm for both models of the cyclone separator. It is observed that the new design collects higher number of particles compared to the mathematical model. Evidently, the flow pattern results show that a higher number of particles are trapped in the collection bin of optimum design cyclone compared with the mathematical model. Moreover, the highest number of particles are swirling at the conical section of the optimum design cyclone compared to the mathematical model. These results clearly show that the optimum design produces better efficiency. The flow pattern results are shown in Fig. 11.

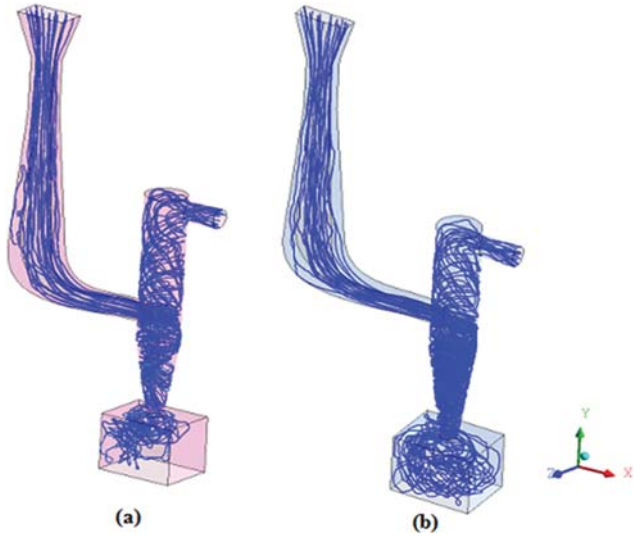

Fig. 11. Flow pattern analysis (particle size of 7 μm): (a) Mathematical model (b) new design.

5. Comparison of Results

The important geometric parameters of the bottom inlet cyclone separator (total height, body height and inlet width of the venturi) were altered by the response surface methodology and particle swarm optimization (PSO). Afterwards, the PSO results were compared with the genetic algorithm (GA) optimization results. These two optimization techniques produce more or less the same results. Based on this optimization results, an experimental setup was created for validating the optimization results. The CFD technique was used for predicting the efficiency, pressure drop and cut-off diameter of the mathematical model and optimum design cyclone. These optimization results are depicting that minimizing the body height of the cyclone and inlet width of the venturi reduces the cut-off diameter. It is noted that the total height of the cyclone remains at the same value for both models of the cyclone separator. The static pressure drop values were found for the different inlet velocities at the inlet of the cyclone. It is noted that the pressure drop of the mathematical model is high when compared with the optimum design for each velocity. The inlet velocity versus static pressure drop values of the mathematical model and the new design cyclone are shown in Fig. 12. In addition, the cut-off diameter values were determined for the different inlet velocities, which are depicted in Fig. 13. It is observed that the increasing the inlet velocity at the inlet of the venturi decreases the cut-off diameter. Further, it confirms that the cut-off diameter is less in each velocity for the opti-

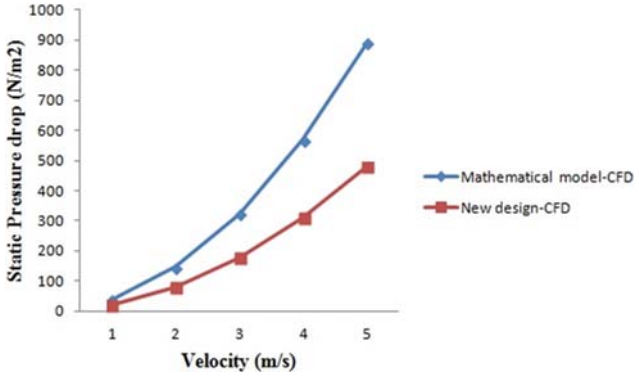

Fig. 12. Velocity vs pressure drop plot.

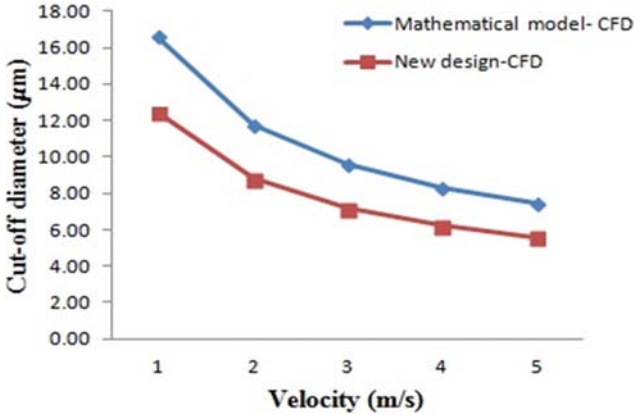

Fig. 13. Velocity vs cut-off diameter plot.

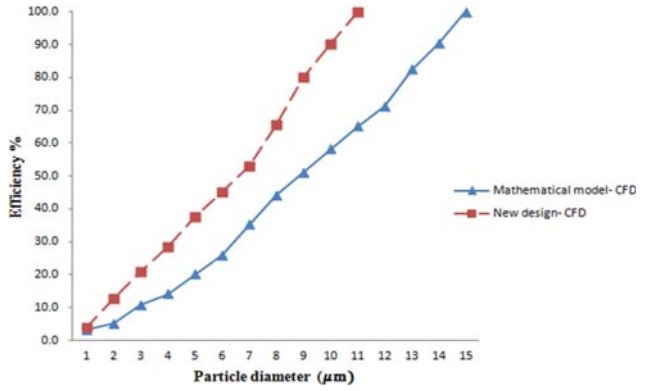

Fig. 14. Particle diameter vs efficiency plot.

mum cyclone when compared with the mathematical model. Next, the efficiency was calculated from each diameter of the particles in CFD by Eq. (11). The particle diameter versus efficiency plot is shown in Fig. 14. The efficiency of the new design plot is high when compared with the mathematical model. The new design collects 100% of the particles at 11 μm and the mathematical model collects 100% of the particles at 15 μm. Moreover, a flow pattern analysis was done by the discrete phase model particle tracking method in CFD. The flow pattern results were obtained for the particle size of 7 μm for both models of cyclones. This result shows that the new design trapped a large number of particles compared with the mathematical model. The comparison results are given in Table 7. It is noted that the cut-off diameter and Stokes number values were calculated at a velocity of 3.3 m/s in mathematical, GA and PSO. The cut-off diameter and Stokes number were estimated at a velocity of 3.9 m/s in experimental and CFD analysis for the new design.

These results were compared with the results of the venturi inlet tangential entry cyclone. Venkatesh and Sakthivel [34] examined the effect of cut-off diameter and pressure drop in venturi inlet tangential entry cyclone separator by numerical and optimization approach. In that analysis, the predicted cut-off diameter for the optimized design is 14.7 μm and Stokes number is 0.013448. Although, the present study produces less cut-off diameter and Stokes number when it is compared with the tangential entry cyclone. This result indicates that the bottom inlet cyclone gives higher collection efficiency comparisons with the venturi inlet tangential entry cyclone separator. The comparative results of the mathematical model, PSO, GA, experimental and venturi inlet tangential entry cyclone are given in Table 7.

CONCLUSION

The optimization of the geometrical parameters of the bottom inlet cyclone separator gave the following results:

- Reducing the size of venturi-inlet width diminishes the cut-off diameter and increases the venturi-inlet width as well enhancing the cut-off diameter.
- Furthermore, increasing the total height and body height of the cyclone also decreases the cut-off diameter.
- Adopting the venturi with bottom inlet cyclone separator reduces the inlet velocity of the particles. Reducing the inlet velocity also reduces the pressure drop between inlet and outlet of the cyclone separator. Due to this less pressure drop, the collection efficiency was improved.
- This research confirms that the genetic algorithm (GA) and particle swarm optimization (PSO) give the same results.
- The experimental result confirms that 50% of the particles are collected at 7 μm particle size, which is better when compared with the mathematical model and venturi inlet tangential entry cyclone. The cut-off diameter of the mathematical model is 9.129 μm, and the cut-off diameter of the venturi inlet tangential entry cyclone is 14.7 μm.
- The Stokes number of the optimized model is less when compared with the mathematical model and venturi inlet tangential entry cyclone.
- Based on these results, one can conclude that the performance of the optimized bottom inlet cyclone is better when compared with the mathematical model in collecting the smaller size magnesium particles.

NOMENCLATURE

D_e : outlet diameter [m]
D : cyclone diameter [m]
B_c : cone tip diameter [m]
h : body height [m]
H_t : total height [m]
a_v : inlet length of venturi [m]
b_v : inlet width of venturi [m]
h_c : convergent section height (h_c)
h_d : divergent section height (h_d)
h_t : throat section height (h_t)

Table 7. Comparison of results

Model	Dimensions (m)			X_{50} (μm)	Stk
	H_t	h	b_v		
Venturi inlet tangential entry cyclone (Venkatesh and Sakthivel (2017)	0.4	0.2	0.041	14.7	0.013448
Mathematical model (Bottom inlet)	0.6	0.4	0.075	9.129	0.01422
PSO	0.6	0.35	0.04	6.84	0.007986004
GA	0.59619	0.35919	0.0401	6.83	0.007962432
Experiment	0.6	0.35	0.04	7	0.008363
CFD	0.6	0.35	0.04	6.9	0.00960

a_t : throat length (a_t)
b_t : throat width (b_t)
H_v : total height of the venturi (H_v)
ρ_p, ρ_g : particle density, fluid or gas density [kg/m^3]
V_i : inlet velocity [m/s]
Stk_{50} : Stokes number
N_e : number of turns
μ : fluid viscosity [kg/ms]
X_{50} : cut-off diameter of the particle [m]
β_o, β_i, β_{ii}, β_{ij} : regression coefficients for intercept, linear, quadratic and interaction terms
X_i, X_j : independent variables
Y : response variables
$c_{1, C2}$: learning factors
R_1, R_2 : random numbers
y_i^n : position vector
v_i^n : velocity vector
P_{ij}^n, g_{ij}^n : pbest and gbest values
w_U, w_L : upper and lower limits of the inertia weight
I_U : maximum number of iterations

REFERENCES

1. W. Peukert and C. Wadenpohl, *Powd. Technol.*, **118**, 136 (2001).
2. R. K. Sinnott, Chemical engineering design, Elsevier Science, Oxford (2005).
3. M. B. Ray, P. E. Luning, A. C. Hoffmann, A. Plomp and M. I. L. Beumer, *Int. J. Miner. Process.*, **53** 39 (1998).
4. A. L. Liu, Y. H. Zhang and L. Ma, *Korean J. Chem. Eng.*, **35**, 1380 (2018).
5. S. Bernardo, M. Mori, A. P. Peres and R. P. Dionisio, *Powder Technol.*, **162**, 190 (2006).
6. T. G. Chuah, J. Gimbun and T. S. Y. Choong, *Powder Technol.*, **162**, 126 (2006).
7. Y. F. Diao, X. Li and P. D. Gu, *Korean J. Chem. Eng.*, **26**, 879 (2009).
8. J. C. Kim and L. W. Lee, *Aerosol. Sci. Technol.*, **12**, 1003 (1990).
9. F. Qian, J. Zhang and M. Zhang, *J. Hazard. Mater.*, **136**, 822 (2006).
10. J. Jiao, Y. Zheng, G. Sun and J. Wang, *Sep. Purif. Technol.*, **49**, 157 (2006).
11. Y. Park, C. Y. Yun and J. Yi, *Korean J. Chem. Eng.*, **22**, 697 (2005).
12. K. Elsayed and C. Lacor, *Comput. Fluids.*, **68**, 134 (2012).
13. A. Avci and I. Karagoz, *International Commun. Heat. Mass. Trans.*, **28**, 107 (2001).
14. B. Zhao and Y. Su, *Chem. Eng. Res. Des.*, **88**, 606 (2010).
15. K. Elsayed and C. Lacor, *Chem. Eng. Sci.*, **65**, 6048 (2010).
16. H. Safikhani, M. A. Akhavan-Behabadi, N. Nariman-Zadeh and M. J. Mahmood Abadi, *Chem. Eng. Res. Des.*, **89**, 301 (2011).
17. S. Pishbin and M. Moghiman, *Chem. Eng.*, **2**, 686 (2010).
18. K. Elsayed and C. Lacor, *Powder Technol.*, **217**, 84 (2012).
19. W. P. Martignoni, S. Bernardo and C. L. Quintani, *Braz. J. Chem. Eng.*, **24**, 83 (2007).
20. V. Kumar and K. Jha, *Sep. Purif. Technol.*, **215**, 25 (2019).
21. R. D. Luciano, B. L. Silva, L. M. Rosa and H. F. Meier, *Powder Technol.*, **325**, 452 (2018).
22. L. S. Brar and K. Elsayed, *Sep. Purif. Technol.*, **207**, 269 (2018).
23. P. Singh, I. Couckuyt, K. Elsayed, D. Deschrijver and T. Dhanene, *J. Optim. Theory. Appl.*, **175**, 172 (2017).
24. S. Viswanathan, *Chem. Eng. Sci.*, **53**, 3161 (1998).
25. C. J. Stairmand, *Ind. Eng. Chem.*, **29**, 356 (1951).
26. D. C. Montgomery, Design and Analysis of Experiments, 4th Ed, Wi1ey, New York (1997).
27. J. Kennedy and R. Eberhart, Particle swarm optimization. In: Proceedings of the IEEE International conference on neural networks, Perth (Australia), 1942 (1995).
28. Z. Michalevicz, Genetic algorithms+data structures=Evolution programs, Springer, New York (1992).
29. B. E. Launder and N. Shima, *AIAA J.*, **27**, 1319 (1989).
30. M. M. Gibson and B. E. Launder, *J. Fluid Mech.*, **86**, 491 (1978).
31. S. Fu, B. E. Launder and M. A. Leschziner, Modeling strongly swirling recirculating jet flow with reynolds-stress transport closures, Sixth Symposium on Turbulent Shear Flows, Toulouse, France (1987).
32. B. E. Launder and D. B. Spalding, *Comp. Meth. Appl. Mech. Eng.*, **3**, 269 (1974).
33. Fluent, Inc., Fluent 6.1.22 Users' Guide (2004).
34. S. Venkatesh and M. Sakthivel, *Desal. Water Treat.*, **90**, 168 (2017).